ENVIRONMENTAL RESEARCH
CLIMATE

PURPOSE-LED PUBLISHING™

LETTER • OPEN ACCESS

Underestimation of meteorological drought intensity due to lengthening of the drought season with climate change

To cite this article: Job Dullaart and Karin van der Wiel 2024 *Environ. Res.: Climate* **3** 041004

ENVIRONMENTAL RESEARCH
CLIMATE

OPEN ACCESS

RECEIVED
23 July 2024

REVISED
26 September 2024

ACCEPTED FOR PUBLICATION
30 October 2024

PUBLISHED
8 November 2024

LETTER

Underestimation of meteorological drought intensity due to lengthening of the drought season with climate change

Job Dullaart* and **Karin van der Wiel**

Royal Netherlands Meteorological Institute (KNMI), De Bilt, The Netherlands
* Author to whom any correspondence should be addressed.

E-mail: job.dullaart@knmi.nl

Keywords: droughts, climate change, precipitation deficit, meteorological drought, drought season, natural variability

Supplementary material for this article is available online

Abstract

Meteorological drought may lead to water shortages, which has negative impacts on water-dependent sectors. Whilst there is a wealth of studies on changing drought intensity or frequency due to climate change, much less is known regarding potential shifts in the timing of drought. The purpose of this study is to analyze the timing of the drought season in the Netherlands and climatic changes therein, with a special focus on the onset of the drought season. Based on an analysis of meteorological observations in the Netherlands over the period 1965–2023, we conclude that the Dutch meteorological drought season has extended forward in time. On average, the drought season starts 16 d earlier in the period 1994–2023 compared to 1965–1993. This is mostly the result of an increase in potential evapotranspiration, while the amount of precipitation does not show a clear change at the start of the growing season. Using three climate model ensembles, we show that a forced climate change signal exists, but that natural variability also plays a role. Following this assessment of trends in meteorological variables, we analyze the consequences for the operational monitoring of meteorological drought. In the Netherlands, this is done by means of the 'precipitation deficit'-indicator, based on a fixed-in-time starting point (1 April) of the drought season. The combination of this fixed starting point and the observed earlier onset of the drought season, means that in some years the indicator underestimates drought intensity, and that climatic trends are underestimated. We therefore advocate for an update of the operational drought indicator, such that meteorological drought occurring before 1 April will not be missed.

1. Introduction

The last years, western Europe has seen multiple periods with relatively dry and hot weather conditions (Sluijter *et al* 2018, Bakke *et al* 2020, Philip *et al* 2020, Zscheischler and Fischer 2020, van der Wiel *et al* 2021, 2023, Blauhut *et al* 2022, Rakovec *et al* 2022, Aalbers *et al* 2023). Such periods, with an abnormal precipitation deficit (PD), in relation to the long-term average conditions for a region, are referred to as meteorological drought. When a meteorological drought persists, propagation to agricultural drought (i.e. low soil moisture) and hydrological drought (i.e. low groundwater, streamflow, and lake levels) may occur (Van Loon 2015). Droughts can have major consequences for water dependent sectors (Bartholomeus *et al* 2023). For example, in the Netherlands, reduced crop yields might be the result of too dry conditions, or seawater entering the freshwater system under low river flow (salinization) (Beillouin *et al* 2020, van Oort *et al* 2023). In addition, water use may be constrained for industry and energy supply companies due to increased water temperatures and low flow conditions (van Vliet *et al* 2013, Behrens *et al* 2017), with the latter also hampering shipping (Vinke *et al* 2022). Furthermore, reduced groundwater levels result in peat oxidation and soil subsidence (Schothorst 1977, van Asselen *et al* 2018), and terrestrial and aquatic ecosystems might not be able to cope with drought events (De Boeck and Verbeeck 2011).

Previous studies have assessed whether the intensity and frequency of droughts have changed or are projected to change in relation to anthropogenic climate change. Philip *et al* (2020) assessed trends in summer potential evapotranspiration (PET) and precipitation from 1965 until 2018 for coastal and inland regions (more than 50 km away from the coastline) of the Netherlands. Most importantly, they found a drying trend in the inland region due to a positive trend in PET, while no significant trend was found in precipitation. In addition, van der Wiel *et al* (2023) assessed the occurrence of multi-year droughts in the Rhine basin. They show that in the current climate these occur on average once every fifteen years, with future climate projections indicating a doubling of event probability at 1 °C additional global warming. Finally, the KNMI'23 national climate scenarios (Van Dorland *et al* 2023, van der Wiel *et al* 2024) indicate that summers in the Netherlands will be drier by 2100 under both low- (SSP1-2.6) and high-emission (SSP5-8.5) scenarios. In the high-emission scenario, and considering dry-trending CMIP6 models, current dry summers (5th percentile precipitation deficit) will be average summers by 2100.

In contrast, the timing of the meteorological drought season and climatic changes therein, which contributes to the severity of impacts as well, has not been extensively studied. Here, with the term drought season we mean the period during which PET generally exceeds precipitation. Natural ecosystems and crops are most sensitive to dry weather conditions and reduced soil-moisture availability during the growing season (Zscheischler and Fischer 2020). Rising temperatures and increasing PET, due to climate change, may result in a lengthening of the drought season, of which leaf unfolding advancing forward in spring, and delayed leaf coloring in autumn are notable effects (Myneni *et al* 1997, Menzel and Fabian 1999). A potential earlier onset of the meteorological drought season could be problematic because high demand for water exists at the start of the growing season. In the Netherlands, for example, farmers irrigate their crops to help them grow after planting (European Environment Agency 2021). One study exists that investigated meteorological wet and dry transitions; however, they focused on the Meuse river basin (Hariharan Sudha *et al* 2024). Overall, some studies exist that assessed the length of the Dutch drought season from a biological perspective, but the meteorological perspective is incomplete. Therefore, this study assesses the timing of the meteorological drought season in the Netherlands, with a special focus on its onset.

This manuscript describes our assessment of the magnitude of changes in the timing of the drought season in the Netherlands over the observational period, and to what extent the noted changes are caused by anthropogenic climate change. Given the significance of drought for society, we also discuss the implications for the current operational drought monitoring indicator. The manuscript is outlined as follows: we start with a brief overview of the meteorological drought indicators currently used to inform Dutch water management (section 2) and describe the methodological setup of our analysis (section 3). The results are split up in an analysis of observed changes in the mean annual cycle (section 4.1), a comparison of observed and simulated changes (section 4.2), and the assessment of the implications of the operational drought indicator (section 4.3). In the discussion and conclusions (section 5) we provide a summary and suggestions for improving operational drought monitoring in times of climate change.

2. Operational monitoring of meteorological drought in the Netherlands

The Royal Netherlands Meteorological Service (KNMI) monitors meteorological drought by means of the PD ('neerslagtekort' in Dutch, figure 1(a)). It is calculated as the cumulative difference of PET and precipitation, set to zero if smaller than zero (Philip *et al* 2020), averaged over thirteen weather stations spatially distributed over the country (figure 1(b)). The PD enables the user to put the current meteorological drought season into perspective. For example, in July 2024 the PD was far below the median, indicating relatively wet circumstances. The equation of PD is given by:

$$PD_t = \max\{0,\ PD_{t-1} + (PET_t - P_t)\}$$

$$\text{with } PD_{t=0} = \max\{0,\ (PET_{t=0} - P_{t=0})\}$$

where:

$$t = \textit{days until } 30 \textit{ September},\ \textit{with } t = 0 \textit{ on } 1 \textit{ April}$$

Because climatologically daily values of PET start to exceed precipitation around early April, the PD is calculated from 1 April onwards (Beersma and Buishand 2007). In addition, because global radiation and thus PET decrease in autumn, the PD is calculated until 30 September. This period (1 April–30 September)

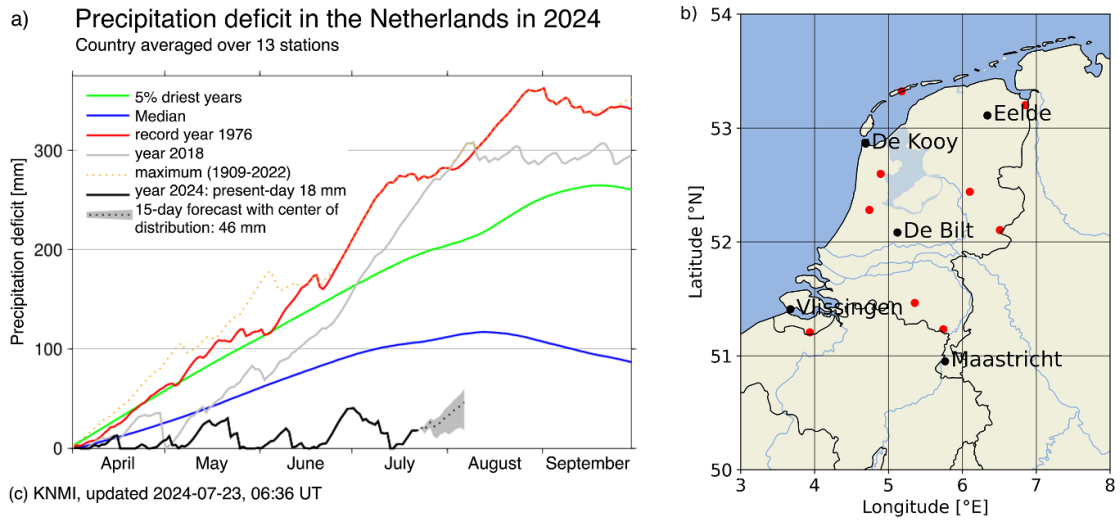

Figure 1. (a) Precipitation deficit in the Netherlands in 2024 as presented by the KNMI on their website for operational drought monitoring purposes (date: 23 July 2024). The black line shows the current precipitation deficit averaged over 13 stations (the 'P13') in the Netherlands. The black dotted line and grey shading show the 15 day forecast based on the ECMWF ensemble forecast. Also shown are the median (blue), fifth percentile (green), maximum over time (dotted orange), record year 1976 (red), and recent dry year 2018 (grey). (b) Map of the Netherlands with the P5 automatic weather stations in black. The red dots indicate the locations of the KNMI P13 automatic weather stations on which the operational precipitation deficit is based. Except for Maastricht, all P5 stations are also part of the P13.

largely coincides with the growing season in the Netherlands. Because the PD is calculated as a cumulative value over a chosen period, its value depends on the date on which calculations start. Importantly, and the motivation for this study, dry periods before the start date (1 April) are not measured in the operational value of PD. Similarly, climatic changes towards drought before the start date are missed in climatological analyses of PD. For farmers, for example, low precipitation in March makes a big difference on the amount of available soil moisture in the rootzone at the start of the growing season (Philip *et al* 2020) and for that reason an analysis of meteorological drought before 1 April might be of value.

Also other common indicators of meteorological drought used around the world, e.g. standardized precipitation index (SPI; Mckee *et al* 1993) and Standardized Precipitation Evapotranspiration Index (SPEI; Vicente-Serrano *et al* 2010), cannot be used to assess changes in the length of the meteorological drought season. SPI-n (and similarly SPEI-n) is a statistical indicator comparing the total precipitation received during a period of n months with the long-term precipitation distribution for the same period (e.g. SPI-1, SPI-3, SPI-6, SPI-12, etc). Because of the use of a fixed period, here n months at different start dates in the calendar year, these indices are not suitable to detect a possible lengthening (or shortening) of the drought season and consequences of that on intensity changes. Instead, to be able to study meteorological drought on a daily basis we make use of the PD as indicator.

3. Materials and methods

The methodology is illustrated in figure 2. To assess whether the Dutch drought season is starting earlier we compare climatological mean values of temperature, precipitation, global radiation, and PET over 1965–1993 against 1994–2023 (section 3.1) centrally in the Netherlands (De Bilt), and at four other KNMI weather stations with a good spatial representation of the Netherlands. Furthermore, to assess to what extent the observed climatic changes are related to climate change or natural variability we compare observations against three climate model ensembles (section 3.2). Finally, to assess whether the PD is still a suitable metric for drought analysis in the Netherlands we adjust the start date in the indicator calculation and compare results (section 3.3).

3.1. Historical observations

We use observational data from five automatic weather stations (AWS) around the Netherlands to analyze changes in drought timing in the period 1994–2023 compared to 1965–1993. Daily values of temperature (°C) and global radiation (W m^{-2}) are obtained from AWS. Precipitation (mm d^{-1}) is measured at a network of rain gauges operated by volunteers. We refer to this set of five AWS and nearby rain gauges as the P5 (table 1 and figure 1(b)). Values of PET are computed based on the formula of Makkink (Makkink 1957). For the analysis, we first compute a daily climatology by taking the average over the period of interest. As a

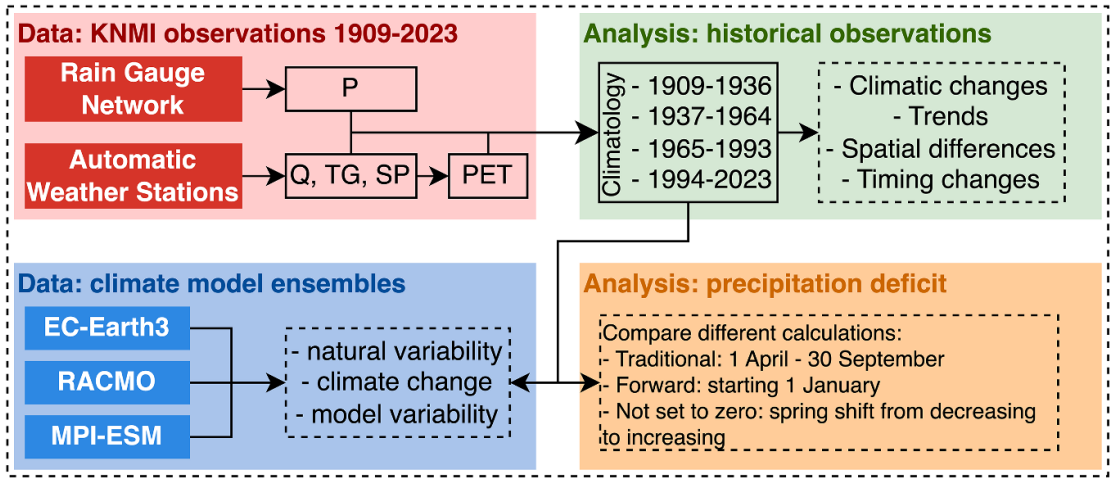

Figure 2. Flowchart of the research framework showing the observations (red), analysis of the historical data (green), climate model ensemble data and analysis (blue), and precipitation deficit analysis (orange). The symbols represent precipitation (P), global radiation (Q), daily mean temperature (TG), relative sunshine duration (SP), and potential evapotranspiration (PET).

Table 1. Overview of KNMI AWS and rain gauge stations that are used in this study to which we refer as the P5. The station number is indicated between brackets.

Automatic weather station	Coordinate	Rain gauge station	Coordinate
De Bilt (260)	5.2 E 52.1 N	De Bilt (550)	5.2 E 52.1 N
De Kooy (235)	4.8 E 52.9 N	De Kooy (025); Den Helder before 1972 (009)	4.8 E 52.9 N; 4.8E 52.9 N
Eelde (280)	6.6 E 53.1 N	Groningen (139)	6.6 E 53.1 N
Maastricht (310)	5.8 E 50.9 N	Roermond (961)	5.7 E 50.8 N
Vlissingen (380)	3.6 E 51.4 N	Kerkwerve (737)	3.6 E 51.1 N

second step, to remove noise and better expose the signal of the underlying causal processes, we smooth the data by taking the 60 day centered running mean.

Observations started earlier than 1965, and for parts of this study we use the entire dataset. Before 1965, global radiation was not measured directly at all the P5 stations. Instead, for these years we compute global radiation based on temperature and the percentage of maximum potential sunshine duration (SP) using a set of location dependent formulas of Frantzen and Raaff (1982). Data is obtained starting in 1909, because from this year onwards SP (%) is measured continuously at the P5. In the supplement we provide a full description of the observational dataset, changes therein over time, and where the data is available (supplementary note 1).

3.2. Climate model ensembles

Observed historic trends are influenced by both the forced anthropogenic climate trend and natural climate variability. To determine the driver(s) of the observed trend we compare the observed changes against simulated changes in three climate model ensembles (initial-condition ensembles, Deser *et al* 2020). The output of two GCMs and one downscaled RCM will be analyzed (table 2). The output of the RCM (RACMO2v3) is first interpolated from a curvilinear grid to a regular lon/lat grid with a resolution of $0.1° \times 0.1°$. Subsequently, for each of the ensembles we use the grid cell in which De Bilt is located. In terms of PET the climatology of the three climate model ensembles is in good agreement with observations at De Bilt (figure S1), while observed precipitation is much more equally distributed over the year compared to what is shown by the climate model ensembles. A RACMO-PGW simulation (Aalbers *et al* 2023) (with ERA5 as boundary condition) shows a yearly precipitation pattern for 1994–2023 that is very similar to observations in De Bilt (figure S1(d)). This shows that it is most likely the large-scale circulation that is not correctly captured by the global climate models (EC-Earth3 and MPI-ESM1.2), resulting in a large bias in the yearly precipitation pattern over the Netherlands.

Table 2. Overview of the climate model ensembles used in this study. The columns indicate the name, type (regional or global), the member-size, and the spatial resolution of each model, respectively.

Climate model	Type	Members	Spatial resolution
MPI-ESM1.2 (Gutjahr *et al* 2019)	GCM	30	$1.875^\circ \times 1.875^\circ$
EC-Earth3 (Döscher *et al* 2022)	GCM	16	$0.70^\circ \times 0.70^\circ$
RACMO2v3 (Van Meijgaard *et al* 2008)	RCM (boundary forcing from EC-Earth3)	16	$0.11^\circ \times 0.11^\circ$

3.3. Analyses

To assess whether the Dutch drought season is starting earlier we compare climatological mean values of temperature, precipitation, global radiation, and PET in De Bilt over 1965–1993 against 1994–2023, and at four other KNMI weather stations with a good spatial representation of the Netherlands. The climatological mean values are the daily means over the two time periods, which are smoothed by computing the 60 day centered mean. The mean value on 1 April in 1965–1993 is taken as a threshold and we check how many days earlier (or later) this value in exceeded in 1994–2023. In addition, to gain more insight into natural variability the analysis is extended with the periods 1909–1936 and 1937–1964.

We also assess whether the definition of the PD indicator is of influence in calculation of drought intensity and climatic trends. The PD is traditionally calculated from 1 April until 30 September, though an earlier start of the drought season might advocate for an earlier start of this calculation as well. Therefore, we calculate the PD from 1 January until 31 December and assess differences in the results. Additionally, somewhere in spring a transition point exists, where, on average, PET values exceed precipitation amounts. To assess whether this transition point is moving forward in time due to anthropogenic climate change we perform a calculation in which the PD value may become smaller than zero and check on which date the slope transitions from decreasing (precipitation $>$ PET) to increasing (PET $>$ precipitation).

4. Results

4.1. Changes in the annual cycle of temperature, global radiation, PET and precipitation

Temperature, global radiation, and Makkink PET at De Bilt are higher over the period 1994–2023 compared to 1965–1993 (figures 3(a)–(c)). The mean, median, 25th percentile, and 75th percentile increase, which means that the whole distribution is shifting upwards during the drought season. Consequently, certain thresholds are exceeded earlier in the year. For example, the median temperature on 1 April over the period 1965–1993 of 6.6 °C is reached on average 17 d earlier in the period 1994–2023 (table 3). For global radiation and PET, we observe a forward shift of 7 and 8 d, respectively. To assess whether the increase in PET is mostly influenced by the increase in temperature or in global radiation, we compute PET again using the median values of temperature and global radiation from each period (supplementary figure S2). This shows that the increase in global radiation accounts for about 70% of the increase in PET (39 mm yr^{-1}), while the other 30% is caused by higher temperatures (16 mm yr^{-1}).

Comparing time series of mean temperature, global radiation, and PET that go further back in time (supplementary materials figures S3(a)–(c)), reveals that the changes did not occur linearly in time and that the largest changes occurred in the most recent period. This has multiple causes, greenhouse gas forcing and global temperature did not increase linearly over this period, natural climate variability contributes to the changes, and finally, global radiation is influenced by aerosol forcing. Indeed, global radiation was lower over 1965–1993, compared to 1909–1936, and 1937–1964, also affecting PET. This can be explained by the post-war industrialization and series of volcanic eruptions around 1980 and the eruption of Mount Pinatubo in 1991 (Ohvril *et al* 2009), which increased the aerosol concentration causing more sunlight to backscatter, thereby reducing the amount of radiation that reached the Earth surface (aerosol cooling). Over 1994–2023, the air quality substantially improved over Europe (Markowicz *et al* 2022), leading to higher values of global radiation.

Comparing the observed temperature shift between the P5 stations (supplementary figure S4) shows that the forward shift is larger at the western coastal stations De Kooy (20 d) and Vlissingen (22 d), compared to the inland stations Eelde (16 d), and Maastricht (15 d). For global radiation, a north-south gradient is visible with a forward shift of 4 and 5 d in the north (De Kooy and Eelde), and a larger forward shift of 8 and 9 d in the south (Vlissingen and Maastricht). The pattern in PET is very similar to global radiation. The shift in De Bilt always falls in the middle of the shifts observed at the other P5 stations (table 3), which indicates that the observations from De Bilt provide a representative view of the climatic changes in the Netherlands.

Precipitation shows a clear increase in the yearly sum (figure 3(d)), with much higher precipitation amounts at the end of summer, in autumn, and in winter. The mean yearly precipitation sum increased from 828 mm over 1965–1993–929 mm over 1994–2023 (+101 mm y^{-1}). However, in the spring season (March,

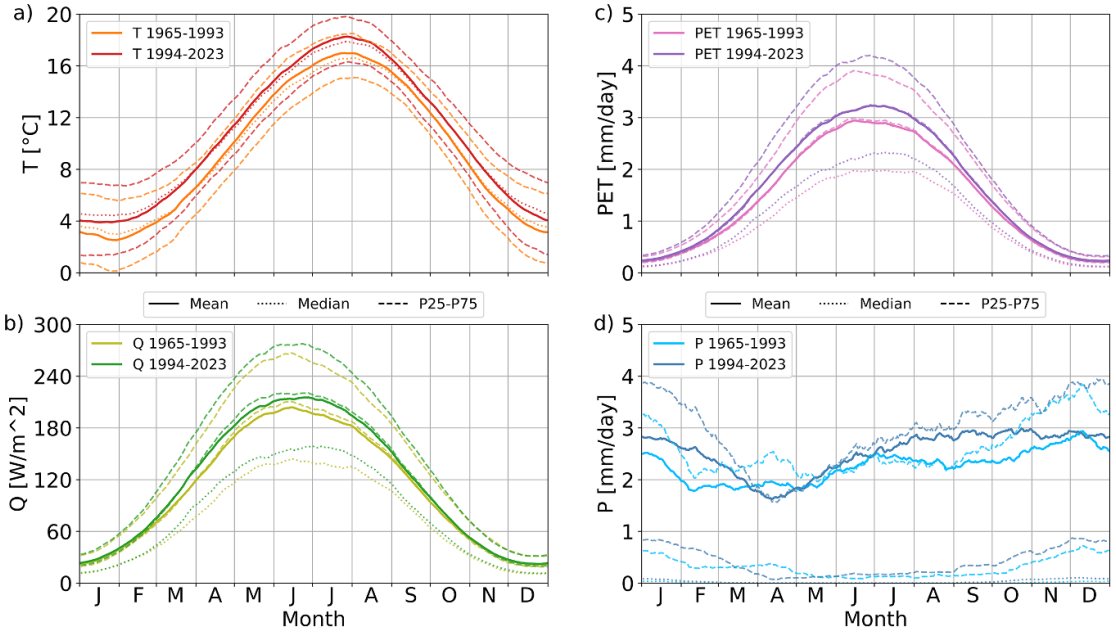

Figure 3. Mean climatology of (a) daily mean temperature (T), (b) global radiation (Q), (c) Makkink PET (PET), and (d) precipitation (P) in De Bilt, Netherlands. Shown are: 60-day running mean (continuous line), median (dotted line), and 25th/75th percentile (dashed lines) over the period 1965–1993 (light colors) and 1994–2023 (dark colors).

Table 3. Temporal shifts in threshold exceedance. The second column shows the threshold considered, the median value of temperature, global radiation, and Makkink PET, at De Bilt on 1 April in the period 1965–1993. The third column shows how many days earlier this threshold value is exceeded in the period 1994–2023. Column four gives the total number of days that the threshold is exceeded over the period 1965–1993, and the last column shows how this changes for the period 1994–2023.

			Length of period above threshold	
	Threshold, median value on 1 April (1965–1993)	Shift in day of threshold exceedance (1994–2023) (Δdays)	1965–1993 (days)	1994–2023 (Δdays)
Temperature	6.6 °C	−16.9	225	+29
Global radiation	121.8 W m^{-2}	−7.4	166	+12
Makkink PET	1.4 mm d^{-1}	−8.3	177	+13

April, and May) only a small increase in precipitation is observed, partly caused by a decrease in April. Time series of mean precipitation that go further back in time (supplementary figure S3(d)), also indicate that precipitation did not increase over the spring season at De Bilt. In line with these results, Ionita *et al* (2020) found a decrease of up to 30 mm in April precipitation over the years 2007–2020, relative to the climatological period 1961–1990 for large parts of western and central Europe. Finally, more so than for temperature and global radiation, large variations in precipitation exist as natural variability is large.

4.2. Comparison of observations and climate model data

Even when looking at differences between two thirty-year averages, the influence of natural variability cannot be disregarded. We therefore use three single model initial-condition large ensembles (SMILEs) (Deser *et al* 2020, Maher *et al* 2021), climate model experiments in which a single model under the same (greenhouse) forcing is used to run different ensemble members that only differ in initial conditions, and hence in internal variability. The spread between the ensemble members provides insight in the magnitude of natural variability. For temperature, for example, all three data sets contain at least one member that shows a backward shift (April 1 threshold exceeded later in the year rather than earlier, figure 4), furthermore, the range of shifts in the data sets exceeds 30 d. Despite this fairly large contribution of internal variability, the median over the members within a data set shows a consistent forward shift for temperature, global radiation, and PET. This indicates that the forced climate response, due to anthropogenic greenhouse gas emissions, indeed leads to a forward shift of higher values for temperature, global radiation, and PET.

For temperature, the observed shift at De Bilt overlaps with the interquartile range (P25–P75) of RACMO2v3 and MPI-ESM1.2 ensembles (figure 4). However, for global radiation, of all members that are part of the three ensemble data sets only 2 out of 62 indicate a forward shift that is larger than what is

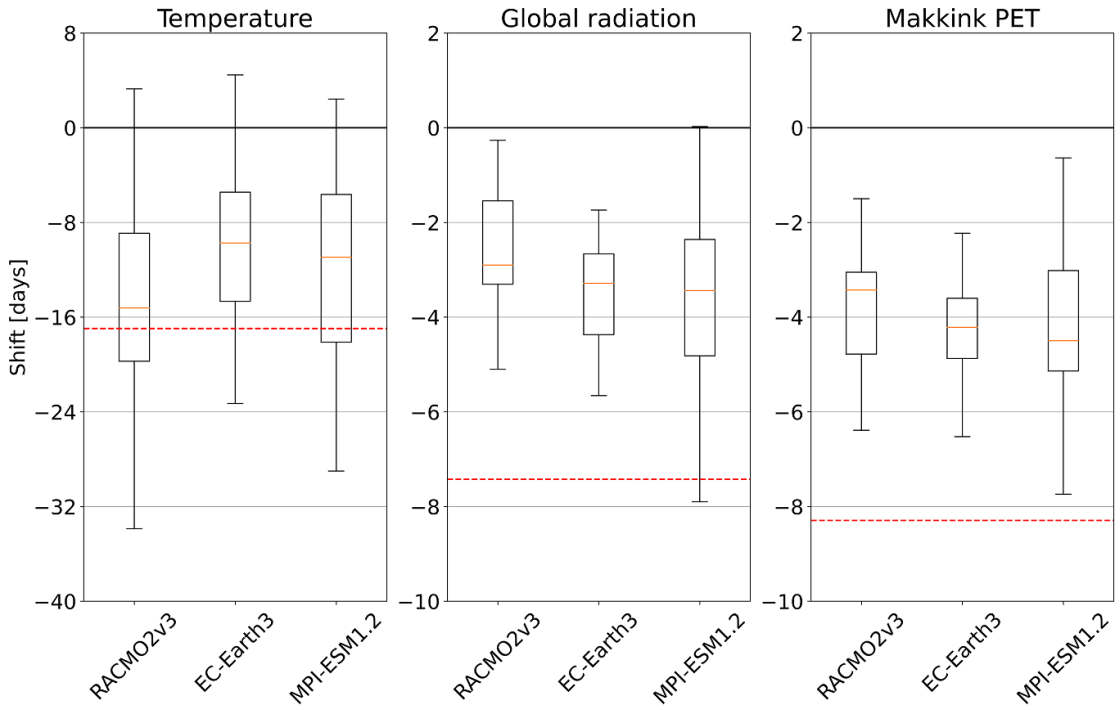

Figure 4. Boxplot indicating the shift in the day of the year on 1 April threshold value (over 1965–1993) is exceeded over the period 1994–2023. Results are shown for RACMO2v3, EC-Earth3, and MPI-ESM1.2, that consist of 16, 16, and 30 members, respectively. Dashed red line shows the observed shift at De Bilt (table 3). The box extends from the first quartile to the third quartile of the data, with an orange horizontal line at the median. The whiskers extend from the box to the farthest data point lying within 1.5x the inter-quartile range from the box.

observed. For PET, none of the ensemble members shows a forward shift that is as large as observed. This discrepancy between climate model output and observations could be an indication that the observed trends are dominated by large internal variability. However, it could also be that the climate models do not capture the effects of increased greenhouse gases and changing aerosol loads on global radiation (and PET). As discussed in the previous section, the strong reduction in aerosol emissions in Europe since the 1980s has caused a significant increase in incoming surface shortwave radiation. When the climate models do not take this decrease in aerosol concentrations into account, they will not be able to capture the increase in global radiation since the 1980s (Chen 2021, Schumacher *et al* 2024). All climate models used in this study consider an anthropogenic time-varying spatially uniform aerosol forcing. However, for the same aerosol forcing, different models can simulate very different aerosol concentrations, hence producing different radiative forcing (Haarsma *et al* 2016). Alternatively, a bias in the simulation of clouds could also be the cause of this discrepancy between observed and simulated global radiation.

4.3. Implications for the Dutch meteorological drought indicator: PD

In this final section we review the consequences of the observed forward shift in PET on the use of PD as a metric for operational monitoring of meteorological drought. Calculating the PD from 1 January onwards, rather than 1 April as is normally done (see Methods), reveals that the typical time of increasing PD in spring also advances forward (figure 5(a)). The difference in the PD between the two periods (1965–1993 and 1994–2023) stays relatively constant from mid-April until July. The climatological mean peak PD value, around 31 August, lies 6 mm higher in the second period. From September onwards the observed increase in precipitation over the second period causes the PD to decrease more quickly compared to the first period.

Next, we compute the PD without setting it to zero when it becomes smaller than zero (figure 5(b)). This way, the PD shows a transition point at which PET, climatologically, exceeds precipitation, which may be used as an indicator of the start date of the drought season. In 1965–1993 this transition point falls on 19 April, in the period 1994–2023 this is 16 d earlier on 3 April (black dots in figure 5(b)). When looking at the median instead of the mean a similar forward shift is found of 16 d (from 24 April to 8 April). A forward shift in the climatological values (mean/median) is also observed at De Kooy (7/4 d), Eelde (19/9 d), Vlissingen (15/9 d), and Maastricht (22/24 d). Note that these are climatological mean values and that there is quite some variability in the timing of the transition point. For years in which the transition point falls before the start of the PD calculation, the resulting values of PD are influenced.

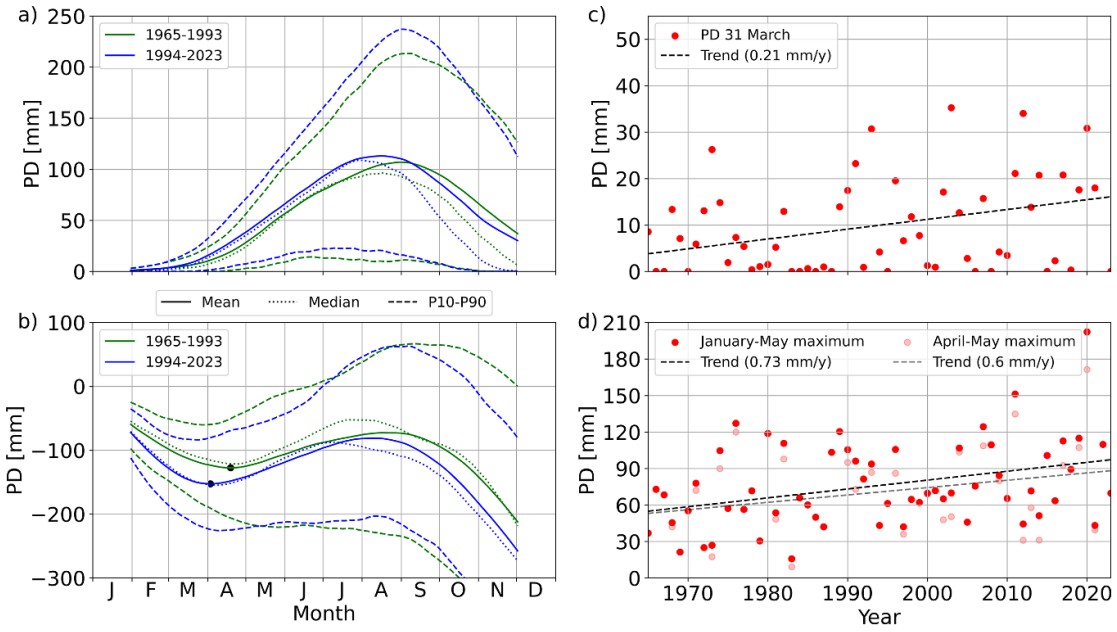

Figure 5. (a), (b) 60 day running mean (continuous line), median (dotted line), and 10th/90th percentile (dashed lines) over the period 1965–1993 (green) and 1994–2023 (blue) of the PD computed (a) starting 1 January, and (b) starting 1 January, and allowing negative values. The forward shift is depicted by the black dots that represent the transition point from decreasing to increasing. (c) PD value on 31 March, with PD calculated as in (a). (d) Maximum value of PD when computed over the period January-May (dark dots) and when computed over the period April–May (light dots) per year. Dashed lines in (c), (d) show a linear trend line.

To quantify this effect, the occurrence of drought and changes therein before 1 April, we compute, for each year, the PD value starting from 1 January and analyze its value on 31 March (figure 5(c)). This shows that the PD is often larger than zero on 31 March with a mean and median value over the years 1965 until 2023 of 10 mm and 6 mm, respectively. Consequently, by starting the current operational calculation on 1 April, following the assumption that on this date the PD is zero, may result in an underestimation of the actual PD at that time and further in the season. Furthermore, the PD value on 31 March shows an upward trend of 0.21 mm yr^{-1}, mainly caused by increasing PET. Excluding the very dry spring of 2022 with a PD of 52 mm on 31 March results in a smaller but still substantial trend of 0.15 mm yr^{-1}, indicating that the trend is robust. In certain years, a large PD value on 31 March may be cancelled (PD reset to zero) when the following months are wet, in such a case a dry start of early spring might not be problematic. To assess the impact of the starting date of the PD calculation, we determine the intensity of spring drought from PD calculated over January–May and over April–May, drought intensity is measured by the maximum of PD in these periods (figure 5(d)). In general, we observe an increase over time of the intensity of spring drought. This increase, or the upward trend in the maximum PD, is larger when PD is calculated from 1 January (trend = 0.73 mm y^{-1}) than when the calculation starts at 1 April (trend = 0.60 mm y^{-1}). Finally, the difference between these two trends of 0.13 mm y^{-1} is smaller compared to the previously observed trend in the PD on 31 March of 0.21 mm y^{-1}, which shows that indeed, in certain years, the PD observed on 31 March is reset to zero in the period afterwards. Though, in most years, a higher PD at the end of March continues to influence the value of PD in the months afterwards.

5. Conclusion and discussion

Based on an analysis of meteorological observations in the Netherlands over the period 1965–2023, this study shows that the Dutch meteorological drought season has extended forward in time due to anthropogenic climate change. Certain thresholds of temperature, PET, and global radiation are exceeded earlier in the year (table 3), which, combined with no changes in precipitation in the months March, April, and May (table 3(d)), results in a higher chance of meteorologically dry conditions in spring (figure 5(d)). On average, the drought season starts 16 d earlier in the second half of the observed period than the first half (figure 5(b)), and interestingly (though not relevant to our main conclusions), also ends earlier due to the increase in precipitation at the end of summer. These findings are in agreement with Hariharan Sudha *et al* (2024), who found that the drought season start moved forward from mid-April to the end of March over the Meuse river basin between 1951 and 2022. Using three climate model ensembles, we have shown that a forced

climate change signal exists, but that natural variability also plays a role (figure 4). Following this assessment of trends in meteorological variables, we then analyzed the consequences for the operational monitoring of meteorological drought, which at KNMI is done by means of the 'precipitation deficit'-indicator (PD), based on a fixed-in-time starting point of the drought season (see Methods for the detailed definition).

Based on these results, we advocate for an update of the operational PD calculation method at KNMI. The reason for this is twofold: (1) meteorological drought may occur before 1 April. When this happens, this is not taken into account in current operational drought monitoring (as in figure 1), with a potential underestimation of meteorological drought intensity as a consequence (figure 5(d)); and (2) anthropogenic climate change has caused an upward trend of 0.13 mm yr^{-1} of PD in the months January-March, additional to the 0.60 mm yr^{-1} trend that is found in maximum PD in April-May (figure 5(d)). As such, climatological analyses based on the current indicator underestimate the real trend in drought intensity. In general, the assumption that the PD is zero at the end of March is not valid, and this discrepancy has become larger due to climate change (figure 5(c)). Though the analysis has focused on the Dutch drought indicator, other fixed period meteorological drought indicators (e.g. SPI and SPEI) cannot be used to assess changes in the length of the drought season. Starting the PD calculation earlier in the year, for example in January, will make sure that the possible start of the drought season before 1 April will not be missed.

The analysis in this paper is based on observations from a limited set of five KNMI AWS and rain gauge stations. Using a larger set of weather stations may improve the robustness of results in terms of spatial patterns and natural variability. This could be achieved by using data from more KNMI stations or by extending the analysis to neighboring countries such as Germany and Belgium. However, the choice for this set of P5 weather stations was made because the time series of all variables of interest are almost complete from 1909 onwards. In addition, global radiation was measured at these AWS from 1965 onwards, while at most other KNMI AWS direct measurements of global radiation started only after 1990. The observations in De Bilt, located centrally in the Netherlands, consistently fall in between the observations from the P5 stations, giving confidence in the quality of the observations and the results.

Second, it remains unclear whether the recent very dry spring and/or summer seasons in 2018, 2019, 2020, and 2022 are part of a strong upward trend in the frequency of meteorological drought events or if natural variability is their main cause. Analyses of climate modeling experiments are the obvious way to address this question but are somewhat hampered by much lower simulated increases in global radiation in spring than what was observed in these recent summers, something that was also recognized in the KNMI'23 national climate scenarios for the Netherlands (Van Dorland *et al* 2023). This means that either the climate models underestimate the sensitivity of global radiation to increased greenhouse gas concentrations (e.g. due to biases in the simulation of clouds), they miss or underestimate other relevant processes (e.g. changes in aerosol load), or the last few years were truly exceptional. Here, a clear need for further research exists.

Finally, we note that the analysis in this paper deals with the hazard of meteorological drought. Societal risk, e.g. unrecoverable damage in nature, decreased agricultural productivity, or damages to housing due to soil subsidence (Schothorst 1977, De Boeck and Verbeeck 2011, van Vliet *et al* 2013, Behrens *et al* 2017, van Asselen *et al* 2018, Beillouin *et al* 2020, Vinke *et al* 2022, Bartholomeus *et al* 2023, van Oort *et al* 2023), is a product of this hazard and specific vulnerability and exposure. Partially these will depend on the intensity of subsequent agricultural or hydrological droughts (Van Loon 2015). Here, the specifics of the timing of meteorological anomalies are relevant as well. The observational drought monitoring at KNMI discussed in this paper, is part of a larger national monitoring system which also considers soil moisture levels, groundwater tables and river discharge (Rijkswaterstaat 2024).

Overall, climate is changing, with more extreme weather events as a consequence. In the Netherlands, summers are projected to see an increase of droughts and an increase of short-duration convective rainfall events, and winters are projected to see an increase of wet periods (Van Dorland *et al* 2023, van der Wiel *et al* 2024). An anecdotic example of such a future is provided by the weather of 2023, in which a record long period without any rainfall in May and June was followed by very wet months afterwards, making the full year the wettest since 1906 when KNMI began recording rainfall. These new climatic conditions require societal adaptation, improving operational monitoring (e.g. of meteorological drought, as advised in this study) alone will not be sufficient. Adaptation to both drier and wetter weather in the future requires that the people and policy makers of the Netherlands design and apply increasingly flexible water management strategies to limit negative impacts of increasingly extreme (water) conditions (Bartholomeus *et al* 2023).

Data availability statement

The data and scripts that support the findings of this study are openly available in 'Zenodo' at http://doi.org/10.5281/zenodo.12759983 (Dullaart and van der Wiel 2024).

Acknowledgment

The authors thank Jules Beersma, Theo Brandsma, Frank Selten, and Hylke de Vries for helpful discussions on the topic, and Thomas Reerink, and Erik van Meijgaard for providing EC-Earth and RACMO simulations.

Conflict of interest

The authors declare that they have no conflict of interest.

ORCID iDs

Job Dullaart https://orcid.org/0000-0001-9604-3328
Karin van der Wiel https://orcid.org/0000-0001-9365-5759

References

Aalbers E E, Van Meijgaard E, Lenderink G, De Vries H and Van Den Hurk B J J M 2023 The 2018 west-central European drought projected in a warmer climate: how much drier can it get? *Nat. Hazards Earth Syst. Sci.* **23** 1921–46
Bakke S J, Ionita M and Tallaksen L M 2020 The 2018 northern European hydrological drought and its drivers in a historical perspective *Hydrol. Earth Syst. Sci.* **24** 5621–53
Bartholomeus R P *et al* 2023 Managing water across the flood-drought spectrum—experiences from and challenges for the Netherlands *Cambridge Prisms: Water* **1** 1–22
Beersma J J and Buishand T A 2007 Drought in the Netherlands—regional frequency analysis versus time series simulation *J. Hydrol.* **347** 332–46
Behrens P, van Vliet M T H, Nanninga T, Walsh B and Rodrigues J F D 2017 Climate change and the vulnerability of electricity generation to water stress in the European Union *Nat. Energy* **2** 17114
Beillouin D, Schauberger B, Bastos A, Ciais P and Makowski D 2020 Impact of extreme weather conditions on European crop production in 2018: random forest—yield anomalies *Phil. Trans. R. Soc.* B **375** 20190510
Blauhut V *et al* 2022 Lessons from the 2018–2019 European droughts: a collective need for unifying drought risk management *Nat. Hazards Earth Syst. Sci.* **22** 2201–17
Chen L 2021 Uncertainties in solar radiation assessment in the United States using climate models *Clim. Dyn.* **56** 665–78
De Boeck H J and Verbeeck H 2011 Drought-associated changes in climate and their relevance for ecosystem experiments and models *Biogeosciences* **8** 1121–30
Deser C *et al* 2020 Insights from Earth system model initial-condition large ensembles and future prospects *Nat. Clim. Change* **10** 277–86
Döscher R *et al* 2022 The EC-Earth3 Earth system model for the coupled model intercomparison project 6 *Geosci. Model Dev.* **15** 2973–3020
Dullaart J C M and van der Wiel K 2024 Scripts and data for "Underestimation of meteorological drought intensity due to lengthening of the drought season with climate change (https://doi.org/10.5281/zenodo.12759983)
European Environment Agency 2021 Water resources across Europe—confronting water stress: an updated assessment (https://doi.org/10.2800/320975)
Frantzen A J and Raaff W R 1982 *De relatie tussen de globale straling en de relatieve zonneschijnduur in Nederland* (available at: https://cdn.knmi.nl/system/data_center_publications/files/000/071/333/original/WR82-05.pdf?1691578173)
Gutjahr O, Putrasahan D, Lohmann K, Jungclaus J H, von Storch JS, Brüggemann N, Haak H and Stössel A 2019 Max planck institute earth system model (MPI-ESM1.2) for the high-resolution model intercomparison project (HighResMIP) *Geosci. Model Dev.* **12** 3241–81
Haarsma R J *et al* 2016 High resolution model intercomparison project (HighResMIP v1.0) for CMIP6 *Geosci. Model Dev.* **9** 4185–208
Hariharan Sudha S, Ragno E, Morales-Nápoles O and Kok M 2024 Investigating meteorological wet and dry transitions in the Dutch Meuse River basin *Front. Water* **6** 1394563
Ionita M, Nagavciuc V, Kumar R and Rakovec O 2020 On the curious case of the recent decade, mid-spring precipitation deficit in central Europe *npj Clim. Atmos. Sci.* **3** 49
Maher N, Milinski S and Ludwig R 2021 Large ensemble climate model simulations: introduction, overview, and future prospects for utilising multiple types of large ensemble *Earth Syst. Dyn.* **12** 401–18
Makkink G F 1957 Testing the Penman formula by means of lysimeters *J. Inst. Water Eng.* **11** 277–88
Markowicz K M, Zawadzka-Manko O and Posyniak M 2022 A large reduction of direct aerosol cooling over Poland in the last decades *Int. J. Climatol.* **42** 4129–46
Mckee T B, Doesken N J and Kleist J 1993 The relationship of drought frequency and duration to time scales *18th Conf. on Applied Climatology*
Menzel A and Fabian P 1999 Growing season extended in Europe *Nature* **397** 659
Myneni R B, Keeling C D, Tucker C J, Asrar G and Nemani R R 1997 Increased plant growth in the northern high latitudes from 1981 to 1991 *Nature* **386** 698–702
Ohvril H *et al* 2009 Global dimming and brightening versus atmospheric column transparency, Europe, 1906–2007 *J. Geophys. Res.* **114**
Philip S Y, Kew S F, Van Der Wiel K, Wanders N, Jan Van Oldenborgh G and Philip S Y 2020 Regional differentiation in climate change induced drought trends in the Netherlands *Environ. Res. Lett.* **15** 094081
Rakovec O, Samaniego L, Hari V, Markonis Y, Moravec V, Thober S, Hanel M and Kumar R 2022 The 2018–2020 multi-year drought sets a new benchmark in Europe *Earth's Future* **10** e2021EF002394
Rijkswaterstaat 2024 Waterberichtgeving: droogtemonitor (available at: https://waterberichtgeving.rws.nl/owb/droogtemonitor) (Accessed 2 July 2024)
Schothorst C J 1977 Subsidence of low moor peat soils in the western Netherlands *Geoderma* **17** 265–91
Schumacher D L, Singh J, Hauser M, Fischer E M, Wild M and Seneviratne S I 2024 Exacerbated summer European warming not captured by climate models neglecting long-term aerosol changes *Commun. Earth Environ.* **5** 182

Sluijter R, Plieger M, van Oldenborgh G J, Beersma J and de Vries H 2018 *De droogte van 2018* (https://doi.org/10.1016/j.wneu.2018.01.155)
van Asselen S, Erkens G, Stouthamer E, Woolderink H A G, Geeraert R E E and Hefting M M 2018 The relative contribution of peat compaction and oxidation to subsidence in built-up areas in the Rhine-Meuse delta, the Netherlands *Sci. Total Environ.* **636** 177–91
van der Wiel K, Batelaan T J and Wanders N 2023 Large increases of multi-year droughts in north-western Europe in a warmer climate *Clim. Dyn.* **60** 1781–800
van der Wiel K, Beersma J, van den Brink H, Krikken F, Selten F, Severijns C, Sterl A, van Meijgaard E, Reerink T and van Dorland R 2024 KNMI'23 climate scenarios for the Netherlands: storyline scenarios of regional climate change *Earth's Future* **12** e2023EF003983
van der Wiel K, Lenderink G and de Vries H 2021 Physical storylines of future European drought events like 2018 based on ensemble climate modelling *Weather Clim. Extremes* **33** 100350
Van Dorland R *et al* 2023 KNMI national climate scenarios 2023 for the Netherlands *Scientific Report*
Van Loon A F 2015 Hydrological drought explained *Wiley Interdiscip. Rev.* **2** 359–92
Van Meijgaard E, Van Ulft L H, Van De Berg W J, Bosveld F C, Van Den Hurk B J J M, Lenderink G and Siebesma A P 2008 *The KNMI Regional Atmospheric Climate Model RACMO Version 2.1* (KNMI) (https://doi.org/10.1126/science.1153894)
van Oort P A J, Timmermans B G H, Schils R L M and van Eekeren N 2023 Recent weather extremes and their impact on crop yields of the Netherlands *Eur. J. Agron.* **142** 126662
van Vliet M T H, Vögele S and Rübbelke D 2013 Water constraints on European power supply under climate change: impacts on electricity prices *Environ. Res. Lett.* **8** 035010
Vicente-Serrano S M, Beguería S and López-Moreno J I 2010 A multiscalar drought index sensitive to global warming: the standardized precipitation evapotranspiration index *J. Clim.* **23** 1696–718
Vinke F, van Koningsveld M, van Dorsser C, Baart F, van Gelder P and Vellinga T 2022 Cascading effects of sustained low water on inland shipping *Clim. Risk Manage.* **35** 100400
Zscheischler J and Fischer E M 2020 The record-breaking compound hot and dry 2018 growing season in Germany *Weather Clim. Extremes* **29** 100270